

Original Article

# Moore Pseudo Inverse Histology Analysis and Fully Convoluted Watershed Segmentation for Cancer Grading

Peermohamed. A<sup>1</sup>, Sulthan Ibrahim. M<sup>2</sup>

<sup>1</sup>Department of Computer Application, Madurai Kamaraj University (MKU), TamilNadu, India.

<sup>2</sup>Department of Computer Science, Government Arts and Science College, Theni, India.

<sup>1</sup>Corresponding Author : [peermohamed.a003@gmail.com](mailto:peermohamed.a003@gmail.com)

Received: 19 March 2025

Revised: 12 May 2025

Accepted: 23 May 2025

Published: 31 May 2025

**Abstract** - The National Cancer Institute defines histopathological images as the study of diseased cells using a microscope. The pathologist investigates the tissue structure, cell tissue distribution, and cell shape regularities and decides on benign and malignancy in the image. However, the process is found to be more laborious, time-consuming and highly prone to intra and inter-observer variability. To deal with this gap, in this work, a method called, Moore Penrose Pseudo Inverse and Fully Convolution-based Watershed Segmentation (MPPI-FCWS) is proposed. The MPPI-FCWS method is split into two parts, namely preprocessing and segmentation. Initially, the raw histology images obtained from breast histopathology images are subjected to preprocessing using the Moore–Penrose pseudoinverse matrix. Here, normalization and denoising are performed with the objective of identifying metastatic tissue in histopathologic scans of lymph node sections. Second, the process By focusing on the artifacts, the error rate involved in analysis can be reduced. Next, the segmentation of tissues is performed using Fully Convolution-based Watershed Segmentation that focuses on the separation of the region of interest from background tissues as well as the separation of nuclei from cytoplasm, therefore minimizing segmentation error significantly. Experimental evaluation of the proposed MPPI-FCWS method and existing methods are carried out with respect to the number of sample images. The proposed method carries out the experimental evaluation using factors such as precision, recall, accuracy and error rate. The proposed MPPI-FCWS method improved precision and recall by 9% and 31% with a high accuracy rate of 18%.

**Keywords** - Histopathological, Moore penrose, Normalization, Pseudo inverse, Fully convolution, Watershed segmentation.

## 1. Introduction

As far as histology image analysis for cancer diagnosis is concerned, histopathologists investigate the regularities of cell shapes and tissue distributions, make efficient decisions about whether tissue regions are cancerous and accordingly determine the malignancy level manually. Owing to the time-consuming nature and highly susceptible to both intra and inter-observer variability, computer-assisted image analysis is required for quantitative diagnosis of tissue. A histopathological analysis was carried out with pathologists in the diagnosis of breast cancer. Breast Cancer is very predominant for women in today's world. Breast cancer is the second largest disease, which leads to the death of women. The main purpose of breast cancer detection is to identify breast abnormalities as early as possible. The time consumed for detecting breast cancer remained unaddressed. In order to overcome the above issue, a novel proposed method has been developed for classifying breast cancer. T-lymphocyte detection using deep neural networks was proposed in [1] to measure the robustness of marker-labeled lymphocyte quantification algorithms based on the number of training samples prior to and post being transferred to a new tumor

indication. Here, the RetinaNet architecture for the task of cell segmentation and transfer learning was employed to bridge the domain gap between tumor indications and minimize annotation costs for unseen domains. Also, to ensure automatic cell detection and classification, bounding box vertices and class labels were used as annotation databases, therefore improving average precision significantly. Despite improvements observed in terms of average precision, only selected fields of interest were taken into consideration and were never exposed to artifacts during training, therefore causing significant errors. Deep Learning-based Segmentation was presented in [2] for designing an optimized segmentation model. Moreover, an annotation workflow was designed with minimal interference from pathologists on the basis of H&E stained sections. Owing to the reason that immune fluorescence (IF) depends heavily on the proteins in target cells, different types of morphologies were obtained in an optimized manner than human interventions with maximal accuracy. However, the supervised segmentation method is sensitive to biased errors. In fact, training errors and biased errors present major challenges in histology analysis for cancer grading.



Breast cancer is one of the most prevalent malignancies in females globally. A certain extent of benign breast disorders consist of intraductal papilloma, ductal hyperplasia, adenosis and so on. Over recent years, histological examination of specimens has traditionally been utilized under light microscopy in pathological diagnosis. Both early detection and accurate diagnosis with histological segmentation by pathologists are essential for pertinent treatments to boost the patient's prognosis rate. In [3], based on a Single Shot Multibox Detector (SSD), breast carcinoma detection in an automatic fashion was designed.

This mechanism paid more attention to the accuracy aspect. Despite deep learning algorithms achieving an excellent performance using breast cancer histopathological images, however, they were found to be computationally expensive owing to the feature extraction from in-distribution images. In [4], deep-learning-based models for classifying histopathological images and optimization patterns were presented to focus on the computational cost involved in analysis using the dataset from [5]. Yet another method on the basis of image processing technique was presented in [6] to assist pathologists in significantly generating accurate diagnoses by first detecting anomalies using the support vector machine (ADSVM) and resolution adaptive network (RANet) model to perform classification.

This hybrid mechanism ensured both accuracy and computational efficiency. Grading of cancer histopathology slides necessitates large numbers of pathologists and expert clinicians owing to its time consuming nature to look manually into entire slide images. Therefore, an automated classification of histopathological breast cancer is required for performing both clinical diagnosis and therapeutic responses. Over the recent few years, deep learning algorithms for medical image analysis have provided a mechanism for using automated radiologic imaging classification.

In [7], a hybrid method utilizing the convolutional neural network (CNN) and long short-term memory recurrent neural network (LSTM RNN) with the purpose of classifying both benign and malignant breast cancer subtypes was presented in detail. Also this type of hybrid model resulted in the overall performance accuracy in an extensive manner. However, the conventional manual diagnosis requires an in-depth workload and hence is highly susceptible to diagnostic errors.

To address this aspect, a breast cancer histopathology image classification employing multiple compact CNNs was designed [8]. Using this mechanism not only resulted in the workload minimization of pathologists but also boosted the quality of diagnosis extensively. Yet another fusion of CNN employing 1D CNN, 2D CNN and 3D CNN was integrated into [9] to focus on the classification performance. In [10], a deep grade model focusing on the error aspect employing recurrence deep learning was designed.

### 1.1. Research Gap

Currently, several preprocessing, feature selection, and classification methods have been introduced to detect the tumor. Several research works focused on the precision aspect but were unable to concentrate on the accuracy aspect. Conventional preprocessing methods were unable to focus on the overall error. Also, certain research works, though paid focus to recall, compromised on the error rate consumed in cell pattern segmentation with histology analysis for cancer grading. The existing methods need to be improved for healthcare applications that require precise segmentation results. In order to overcome the existing issues, a novel MPPI-FCWS segmentation is introduced.

### 1.2. Novelty and Contributions of the Work

- The proposed MPPI-FCWS method is designed to improve the cancer detection precision rate with a minimal error rate, based on two major processes, namely preprocessing and segmentation.
- The proposed MPPI-FCWS method uses a Statistical Nucleic Normalized Moore Penrose Pseudoinverse Matrix for performing the preprocessing. The novelty of Statistical Nucleic-based Normalization is employed to normalize the image according to the nucleus of cell shape and size. Innovation of the Moore Penrose function for identifying metastatic tissue in histopathologic scans of lymph node sections is applied to minimize the error rate in an extensive manner.
- A fully convolution-based watershed segmentation algorithm is employed in the proposed MPPI-FCWS method for precise cell pattern segmentation with several layers.
- The novelty of the Toeplitz matrix is employed in the MPPI-FCWS method uses convolution for transforming the image and pooling to facilitate dimensionality reduction during kernel size. In this way, precision and recall are enhanced.
- H-minima transform-based Watershed Segmentation is utilized for actual segmentation to provide segmented outcomes. Euclidean Distance Transform is employed for dividing the region of interest from background tissues and separating nuclei from cytoplasm. With this, accuracy is increased.
- A comprehensive experimental assessment is carried out with four different types of performance metrics to illustrate the MPPI-FCWS method over traditional methods.

## 2. Related Works

A fusion DL method was proposed in [11] with the purpose of validating the efficiency and effectiveness of cancer detection. However, as far as biomedical image classification is concerned, acquiring a large training dataset is a demanding task that can be significantly controlled by transfer learning as it acquires the common features from

natural image datasets and can be applied directly to new image datasets. In [12], an efficient deep learning-based computer-aided method for classifying Oral Squamous Cell Carcinoma (OSCC) histopathology images was presented. Employing this hybrid method improved the overall precision and recall values. Owing to the reason that the manual identification procedure is a time-consuming task, it is required to design of an automated mechanism for identifying cancerous and healthy images. In [13], a fusion of the Owl Search Algorithm and DL-Driven Cancer Detection and Classification method was designed. Using the fusion mechanism resulted in the improvement of overall performance.

A review of deep learning methods in breast cancer grading was investigated in [14]. However, with different scales of histopathology, image accuracy is also said to be compromised. A review of work focusing on three scales of histopathology images was detailed in [15]. Though histopathological assessment are said to be the entrenched yardstick for diagnosing breast cancer, it is hindered by time-consuming procedures and hence found to be highly prone to human errors.

A novel approach referred to ImageNet-VGG16 (IVNet) for real-time diagnosis of breast cancer was presented in [16]. Histopathological image analysis in an automatic manner provides a promising solution to boost effectiveness and diagnosis accuracy. In [17], the challenge of breast cancer histopathological image classification by means of ResNet architecture, specifically having the advantage of its depth and skip connections, was presented. By means of these two advantages resulted in the accuracy improvement. A review of histologic grading, with the narration of grading fundamentals, issues related to reproducibility and a detailed discussion on how to enhance reproducibility of grading by training to better recognize mitoses was investigated in [18].

A novel concept employing instance segmentation and object detection for cancer grading was designed in [19]. A detailed analysis of human body cancer detection employing ML and DL techniques, its diagnosis, cure process was discussed in [20]. An extensive study on computer-aided diagnosis employing DL for cancer diagnosis in histopathology images was investigated in [21]. Yet another review of DL in cancer diagnosis was detailed in [22]. A survey of cancer image analysis employing supervised DL was presented in [23]. Computer-aided grading employing DL for pattern classification, focusing on sensitivity, specificity, along with accuracy aspects was designed in [24]. Various traditional deep-learning for making an in-depth analysis of breast cancer histopathological images were proposed in [25]. Also, manual annotation is found to be low-resolution, time-consuming and highly subjected to observer variance. To address this aspect, the H&E Molecular neural network (HEMnet) was designed in [26], therefore producing a higher accuracy. Nevertheless, several research works show extensive inter-observer divergence in breast cancer grading. In [27], deep learning-based breast cancer grading method. An overview of the DL technique focusing on cancer diagnosis and treatment was investigated in [28].

The CNN-based prediction model was developed in [29] for disease diagnosis. However, it failed to achieve greater accuracy while handling large amounts of patient data. A medical IoT-based diagnostic system was employed [30] to determine the difficulty of identifying early-stage breast cancer. But, the time was not focused. With the precise discovery of cancerous patients, an ensemble learning-based voting classifier was developed [31]. Study focused on DL techniques in [32] for improving the diagnostic accuracy. BCR-HDL (Breast Cancer Recurrence using Hybrid Deep Learning) was employed in [33] to predict not only diagnostic outcomes. However, the error was not focused. A comparison of previous existing methods is illustrated in Table 1.

**Table 1. Comparison of previous existing methods reported in the literature**

Reference No	Method	Contribution	Metris	Demerits
[1]	Deep neural networks	Deep neural networks were introduced with T-lymphocyte detection for tumor indication	Average precision was improved	Accuracy was not enhanced
[2]	Deep Learning-based Segmentation	Deep Learning-based Segmentation was employed to optimize the segmentation model	Higher accuracy	Training errors and biased errors present major challenges
[3]	SSD breast carcinoma detection	SSD breast carcinoma detection was performed	Time was lower	Accuracy was not improved
[4]	Deep-learning-based models	Deep-learning-based models were developed to find histopathological images and optimization patterns	Computational overhead was minimized	Precision was not focused
[5]	BReAst Carcinoma Subtyping (BRACS) dataset	BReAst Carcinoma Subtyping (BRACS) dataset was employed for breast cancer	The false positive rate was enhanced	Accuracy was not improved

[6]	Image processing technique	Image processing technique was introduced to help pathologists	Enhanced accuracy and computational efficiency	Precision was not improved
[7]	Hybrid method	The hybrid method was combined with CNN and LSTM RNN to determine breast cancer subtypes	Accuracy was enhanced	Diagnostic errors were not reduced
[8]	CNNs	CNNs were designed for breast cancer histopathology image classification	Improved recall	The quality of the diagnosis was insufficient
[9]	Fusion of CNN employing 1D CNN, 2D CNN and 3D CNN	Fusion of CNN employing 1D CNN, 2D CNN and 3D CNN were combined with classification performance.	Classification accuracy was improved	Error was not minimized
[10]	Deep grade model	Deep grade model was employed for predicting the cancer	Error was reduced	Segmentation was not performed

As discussed in the above literature, though certain research works focused on the accuracy aspect, however paid less attention to the precision factor. Also, some other literature though focused on the recall aspects involved in cancer grading but, paid less attention to the error rate. To address these gaps in this work, MPPI-FCWS is proposed. At first, the Statistical Nucleic Normalized Moore Penrose Pseudoinverse Matrix is utilized for executing normalization and denoising to reduce the error rate. Also, the Fully Convolution-based Watershed Segmentation algorithm is employed via the H-minima transform for analyzing the testing and training sample images. The Toeplitz matrix is used for transforming the image and pooling to facilitate dimensionality reduction. In this way, accuracy, precision, and recall are enhanced.

### 3. Proposed MPPI-FCWS

The detection and classification of breast cancer from histology images are a demanding task due to the reason that an image usually contains many groups and overlapping objects. The various stages involved in the proposed methodology include normalization and, denoising and segmentation of background cells. For the normalization and denoising of the breast cancer histology images, the Statistical Nucleic Normalized Moore Penrose Pseudoinverse Matrix-based preprocessing is used, and for the separation of region of interest from background tissues as well as separation of nuclei from cytoplasm Fully Convolution-based Watershed Segmentation is employed. These models are tested on two fundamental tissues (cancerous or non-cancerous) of randomly selected 1000 breast cancer histology images. Finally, the performances of the proposed MPPI-FCWS are evaluated using well-known parameters, and from the results and analysis, it is observed that the MPPI-FCWS method is performing better for the denoised and segmented features. As illustrated in Figure 1 to start with the breast histopathology images [34] and [35] are acquired as input.

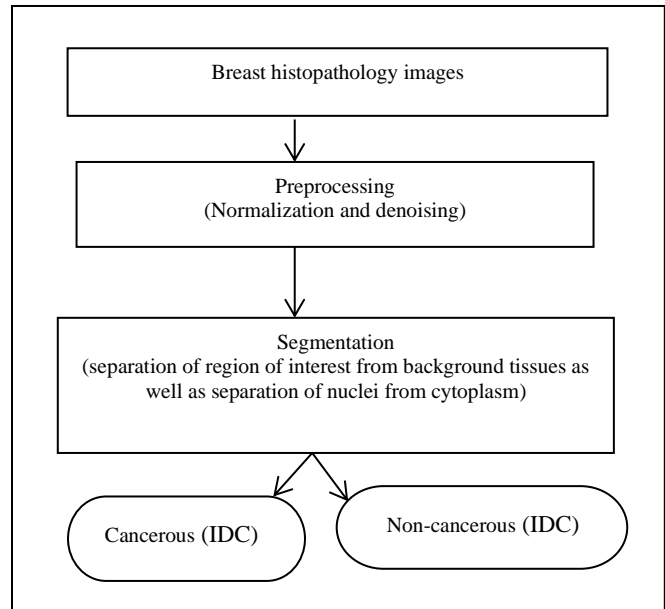


Fig. 1 Flowchart of MPPI-FCWS method

Second, preprocessing is performed using the Moore–Penrose Pseudoinverse matrix. Finally, the segmentation of tissues is done using Fully Convolution-based Watershed Segmentation. The detection and classification of breast cancer from histology images are a demanding task due to the reason that an image usually contains many groups and overlapping objects. The various stages involved in the proposed methodology include normalization, denoising and segmentation of background cells.

For the normalization and denoising of the breast cancer histology images, the Statistical Nucleic Normalized Moore Penrose Pseudoinverse Matrix-based preprocessing is used, and for the separation of region of interest from background tissues as well as separation of nuclei from cytoplasm Fully Convolution-based Watershed Segmentation is employed.

These models are tested on two fundamental tissues (cancerous or non-cancerous) of randomly selected 1000 breast cancer histology images.

Finally, the performances of the proposed MPPI-FCWS are evaluated using well-known parameters and from results and analysis, it is observed that the MPPI-FCWS method is performing better for the denoised and segmented features. A detailed description of the MPPI-FCWS method is provided in the following sections.

### 3.1. Dataset Description

Breast cancer is the most frequent form of cancer in women, and invasive ductal carcinoma (IDC) is the most frequent form of breast cancer. Accurately identifying and classifying breast cancer subtypes is a significant clinical task.

The objective of the breast histopathology dataset acquired from <https://www.kaggle.com/code/paultimothymooney/predict-idc-in-breast-cancer-histology-images> is to identify IDC when it is present in otherwise unlabeled histopathology images.

The dataset comprises 277,524 50x50 pixel RGB digital image patches that were derived from 162 H&E-stained breast histopathology samples. These sample images are small patches that were acquired from breast tissue sample digital images.

Moreover, the breast tissue sample digital images comprise numerous cells; however, only some of them are cancerous. Patches labeled with '1' include cells that are characteristic of invasive ductal carcinoma.

### 3.2. Statistical Nucleic Normalized Moore Penrose Pseudoinverse Matrix-Based Preprocessing

The foremost and principal objective of the preprocessing is to eliminate a definite degradation, including noise reduction or denoising for identifying metastatic tissue in histopathologic scans of lymph node sections.

The breast histopathology images acquired from a microscope may be imperfect and lacking in certain aspects like poor contrast and uneven staining, and they required to be enhanced through a denoising process that, in turn, reduces errors and boosts the overall performance based on cell pattern with histology analysis for cancer grading.

MPPI-FCWS method initially performs color normalization and denoising for identifying metastatic tissue in histopathologic scans of lymph node sections using the Moore–Penrose pseudoinverse matrix. By focusing on artifacts, the error rate involved in analysis can be reduced. As illustrated in Figure 2, with the raw images provided as input, the input image is subjected to preprocessing via normalization and denoising.

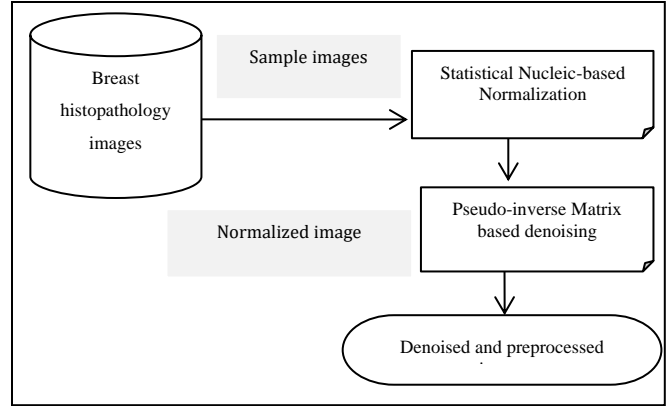


Fig. 2 Based preprocessing model

Let us consider the breast histopathology sample images 'SI', where 'SI ∈ DS' obtained from the raw breast histopathology dataset as input. The average value indicates the centralized tendency of the pixel and is a significant amplitude feature of images. Then, for a breast histopathology sample image 'SI', the average pixel value of each cell pattern is mathematically formulated as given below.

$$f_{mean} = \frac{1}{MN} \sum_{p_c=1}^M \sum_{q_c=1}^N f(p_c, q_c) \quad (1)$$

From the above equation (1), 'f(p<sub>c</sub>, q<sub>c</sub>)', represent the breast histopathology sample image 'SI' pixel value of 'p<sub>c</sub>, q<sub>c</sub>'. Next, with the obtained average pixel value of each cell pattern, Statistical Nucleic-based Normalization is performed in this work. Normalization is utilized in transforming features in the dataset to a common scale, enhancing the overall diagnosis performance and accuracy. The main objective of normalization is to discard the potential biases and distortions caused by numerous feature scales. For breast cancer detection based on cell patterns with histology analysis for cancer grading, histopathologists view the specific features in the cells and tissue structures. Various common features used for breast cancer detection from the microscopic biopsy images include cell size, cell shape, nuclei shape and size and so on. Normalization is performed based on the nucleus of cell shape and size using Statistical Nucleic-based Normalization. The cancer cells' nuclei are larger than the normal cells and divergence from the centre of the mass and hence have to be normalized to discard the possible biases and noises caused by different scales of features. This is performed using statistical functions as given below. First, the nucleus's longest circumference is measured as given below.

$$NLC = f_{mean} [\sqrt{(p_1 - p_2)^2 + (q_1 - q_2)^2}] \quad (2)$$

From the above equation (2), Nucleus Longest Circumference, 'NLC,' is evaluated based on the endpoints on the major axis 'p<sub>1</sub>', 'p<sub>2</sub>', 'q<sub>1</sub>' and 'q<sub>2</sub>' respectively. Second, the nucleus's shortest circumference is measured as given below.

$$NSC = f_{mean}[\sqrt{(p_2 - p_1)^2 + (q_2 - q_1)^2}] \quad (3)$$

From the above equation (3), the Nucleus's Shortest Circumference 'NSC' is measured taking into consideration the endpoints of the minor axis 'p<sub>2</sub>', 'p<sub>1</sub>', 'q<sub>2</sub>' and 'q<sub>1</sub>' respectively. Finally, with the obtained Nucleus Longest Circumference and Nucleus Shortest Circumference values, the abnormality 'Abn' is formulated as given below.

$$NI = Abn = \frac{Majoraxis_{Dis}[NLC]}{Minoraxis_{Dis}[NSC]} \quad (4)$$

From the above equation (4) normalized results are obtained with which denoising is performed using Moore Penrose Pseudoinverse Matrix. We initially assume that the blurring function or point-spread function 'h(n<sub>1</sub>, n<sub>2</sub>)' and the image-denoising methods that are described here fall under the class of linear equations. Under these conditions the denoising process is carried out by means of the Least Square filter. If we denote the blur function as 'h(n<sub>1</sub>, n<sub>2</sub>)', recorded image or the normalized image as 'NI(n<sub>1</sub>, n<sub>2</sub>)' then the noise removed image 'NR(n<sub>1</sub>, n<sub>2</sub>)' is modeled as given below.

$$NR(n_1, n_2) = h(n_1, n_2) * NI(n_1, n_2) \quad (5)$$

$$= \sum_{k_1=1}^{N-1} \sum_{k_2=1}^{M-1} h(k_1, k_2) f(n_1 - k_1, n_2 - k_2) \quad (6)$$

From the above equations (5) and (6), the objective of the image denoising is to make an estimation 'NI(n<sub>1</sub>, n<sub>2</sub>)' of the ideal image, under the assumption that only the degraded image 'NR(n<sub>1</sub>, n<sub>2</sub>)' and the blurring function 'h(n<sub>1</sub>, n<sub>2</sub>)' are given. This is mathematically formulated along with the Pseudoinverse Matrix as given below.

$$NR = hNI; NR \in R^m; NI \in R^n; h \in R^{m*n} \quad (7)$$

$$\begin{bmatrix} NR_1 \\ NR_2 \\ \dots \\ NR_m \end{bmatrix} = \begin{bmatrix} h_1 & h_2 & \dots & h_l & 0 & 0 & 0 \\ 0 & h_1 & \dots & \dots & h_l & 0 & 0 \\ 0 & 0 & h_1 & \dots & \dots & h_l & 0 \\ 0 & 0 & 0 & h_1 & \dots & \dots & h_l \end{bmatrix} \begin{bmatrix} NI_1 \\ NI_2 \\ \dots \\ NI_n \end{bmatrix} \quad (8)$$

With the above said hypothesis as given in equation (7) and Pseudoinverse Matrix as given in equation (8), let 'RM' denote the real matrix with 'm \* n' dimension 'R(RM)' represent the range of 'RM', then the association using Moore Penrose function for identifying metastatic tissue in histopathologic scans of lymph node sections is as given below.

$$RM.NI = b \quad (9)$$

From equation (9) with 'RM ∈ R<sup>m\*n</sup>; b ∈ R<sup>m</sup>', 'b ∉ R(RM)' with an association 'RM.NI = b', then we have 'RM<sup>†</sup>b = Res', where 'Res' denotes the minimal norm solution and 'RM<sup>†</sup>' represents the Pseudoinverse Matrix of

'RM' respectively. Then, the benchmark that we employ for the restoration of blurred images or denoise images is a minimal distance between measured data as below.

$$PI = \min(|NI - NR|) \quad (10)$$

From equation results (10), preprocessed or denoised image 'PI' for identifying metastatic tissue in histopathologic scans of lymph node sections are obtained in an efficient manner.

**Algorithm 1 Statistical Nucleic Normalized Moore Penrose Pseudoinverse Matrix**

Input: Dataset 'DS', Sample Images 'SI = SI <sub>1</sub> , SI <sub>2</sub> , ..., SI <sub>n</sub> '
Output: denoised preprocessed Image 'PI'
Step 1: Initialize 'n'
Step 2: Begin
Step 3: For each Dataset 'DS' with Sample Images 'SI'
//Normalization
Step 4: Evaluate average pixel value of each cell pattern as given in equation (1)
Step 5: Evaluate Nucleus Longest Circumference as given in equation (2)
Step 6: Evaluate Nucleus Shortest Circumference as given in equation (3)
Step 7: Evaluate abnormality to obtain normalized function as given in equation (4)
Step 8: Return normalized image 'NI'
Step 9: End for
//Denoising
Step 10: For each Dataset 'DS' with normalized image 'NI'
Step 11: Formulate image formation using Moore Penrose Pseudoinverse Matrix function as given in equations (5), (6), (7) and (8)
Step 12: Formulate association function as given in equation (9)
Step 13: Obtain preprocessed or denoised image as given in equation (10)
Step 14: Return preprocessed image 'PI'
Step 15: End for
Step 16: End

As given in the above algorithm, with the raw breast histopathology sample images provided as input, the objective remains to reduce the error rate involved in predicting invasive ductal carcinoma (IDC), the most common form of breast cancer. This, in turn, accurately and precisely decides whether tissue regions are cancerous or non-cancerous, therefore minimizing the error rate significantly.

**3.3. Fully Convolution-Based Watershed Segmentation**

Segmentation of nuclei cells is are core analysis step in several histopathology image evaluation tasks. Precise and accurate segmentation forms the fundamental principle of this process. The process consists of the detection of candidate pixels in the preprocessed image and delineation of separation

of the region of interest from background tissues as well as separation of nuclei from cytoplasm by a distinctive criterion employing Fully Convolution-based Watershed Segmentation. Watershed Segmentation, being one of the most popular segmentation techniques, is employed in nuclei and cell segmentation. The algorithm is boosted by specifying local minima only at the regions of interest (ROI) that serve as markers. This Fully Convolution-based marker-controlled watershed has much higher significance in segmenting and separating only these ROI. First, a fully convolutional network is applied that effectively learns to make dense predictions for per-pixel tasks like watershed segmentation. Followed by the

marker selection for watershed segmentation that can be performed in several ways, and in this work, adaptive H-minima transform is used for producing enhanced nuclei shape detection. For H&E-stained images of breast cancer, multiple marker types were utilized for segmentation with the merging of the resulting nuclei segmentations to obtain the final improved combined view. H-minima transform is to differentiate between dark and bright regions of nuclei producing foreground and background markers. As illustrated in Figure 3, for producing precise and accurate tissue and nucleic segmented output, the process is split into two parts, namely, full convolution and watershed segmentation.

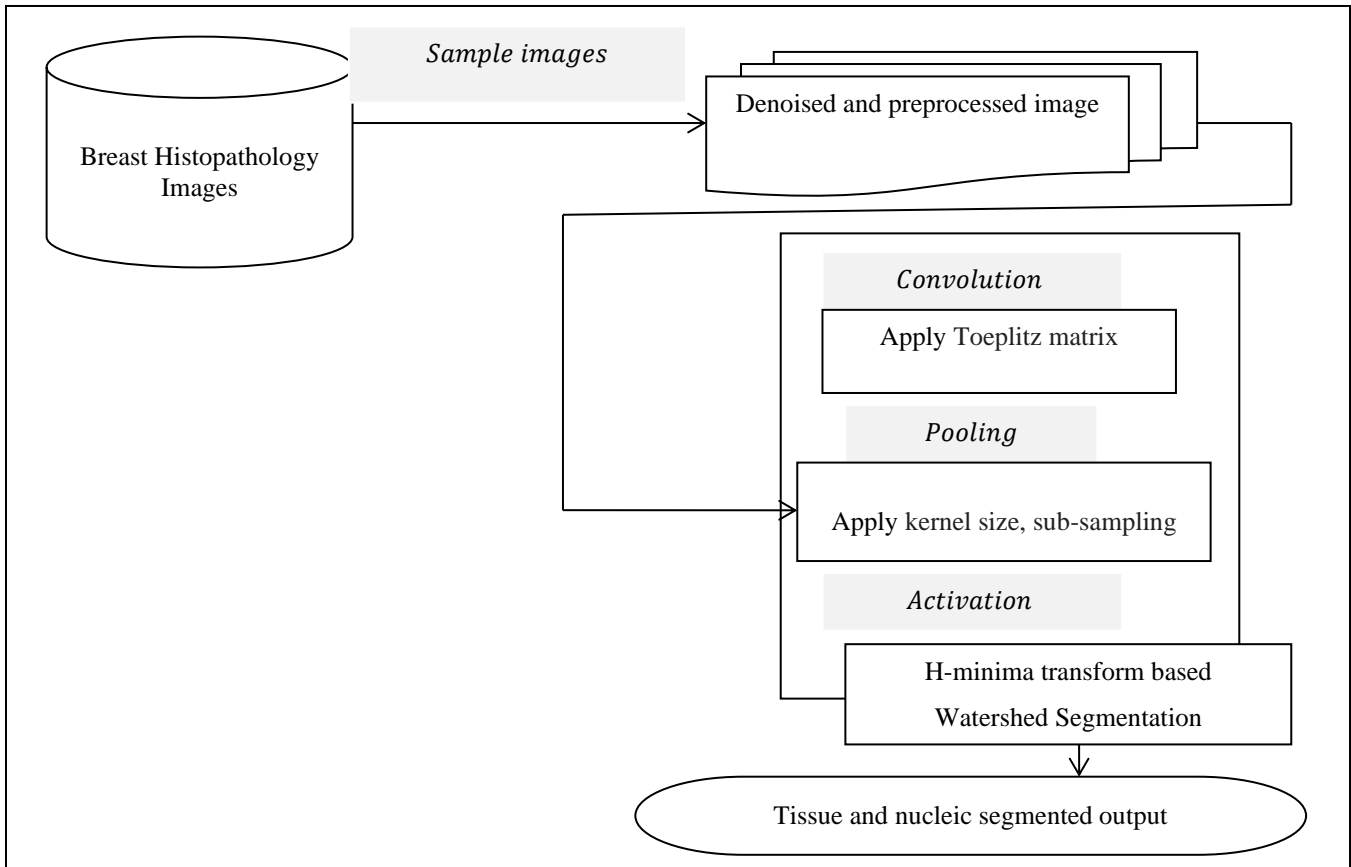


Fig. 3 Block diagram of fully convolution-based watershed segmentation model

First, the preprocessed image provided as input is subjected to the full convolution part, where convolution employing the Toeplitz matrix and pooling with a kernel size of '3 \* 3' is performed to obtain the pooled results. Next, the actual segmentation employing H-minima transform-based Watershed Segmentation is done at the activation part of the full convolution layer, therefore separating the region of interest from background tissues as well as separating nuclei from cytoplasm. Each layer of data in a convnet is a three-dimensional array of size 'x \* y \* z,' where 'xandy' denotes spatial dimensions and 'z' represent the channel dimension. The fully convolutional network consists of convolution, pooling and activation. First, to perform convolution, a

Toeplitz matrix is applied to the sampled preprocessed image 'PI' provided as input. Here, the convolution of two vectors 'PI<sub>i</sub>' and 'PI<sub>j</sub>' represents the area of overlap under the points as 'PI<sub>j</sub>' slides across 'PI<sub>i</sub>'. Convolution is performed by means of the Toeplitz matrix, as given below.

$$Conv = i * j = \begin{bmatrix} i_1 & 0 & \dots & 0 & 0 \\ i_2 & i_1 & \dots & \dots & \dots \\ i_3 & i_2 & \dots & 0 & 0 \\ \dots & i_3 & \dots & i_1 & 0 \\ \dots & \dots & \dots & i_m & i_{m-1} \\ 0 & 0 & 0 & \dots & i_m \end{bmatrix} \begin{bmatrix} j_1 \\ j_2 \\ j_3 \\ \dots \\ j_n \end{bmatrix} \quad (11)$$

$$Pool_{ij} = f_{ks}(\{Conv_{si+\alpha i, sj+\alpha j}\}), 0 \leq \alpha i \leq \alpha j \leq k \quad (12)$$

From equations (11) and (12), convolution ‘Conv’ and pooling operations ‘Pool<sub>ij</sub>’ are performed for two vectors ‘PI<sub>i</sub>’ and ‘PI<sub>j</sub>’ with respect to the sampled preprocessed image ‘PI’. Also, pooling is performed by employing a kernel size ‘k’, sub-sampling ‘s’ that reduces the resolution of the feature map without compromising the contrast. Finally, activation is done using the H-minima transform-based watershed segmentation. The components of the studied H-minima transform-based Watershed Segmentation comprises of 3D marker-controlled watershed ‘WS<sub>MC</sub>’, H-minima-based marker-controlled watershed ‘WS<sub>HMin</sub>’ and connected components ‘CC’ respectively. First, the 3D marker-controlled watershed ‘WS<sub>MC</sub>’ requires an input comprising of markers (i.e., the preprocessed image) and nuclei mask (i.e., the pooled values) and applies Euclidean Distance Transform as below.

$$EDT(i, j) = \sqrt{\sum_{i=1}^n (x_i - adj_i)^2} \quad (13)$$

From the above equation (13), the Euclidean Distance Transform for the two vectors ‘PI<sub>i</sub>’ and ‘PI<sub>j</sub>’ with respect to the sampled preprocessed image, ‘PI’ is obtained based on the image pixel into consideration. ‘x<sub>i</sub>’ and the boundary or adjacent pixel in a binary image ‘adj<sub>i</sub>’ respectively. Followed by the spacings of the transform ‘{space<sub>i</sub>, space<sub>j</sub>, space<sub>k</sub>}’ are normalized to separate regions of interest from background tissues, as given below.

$$\{space_i, space_j, space_k\} = \left\{ \frac{space_{ij}}{space_{ij}}, \frac{space_{jk}}{space_{ij}}, \frac{space_{ki}}{space_{ij}} \right\} \quad (14)$$

Then, Euclidean Distance Transform results and normalized space results, as given in equation (14), are fed to a morphological watershed transform to produce segmentation results that separate nuclei from cytoplasm as below.

$$SRes = WS_{MC}(PI, WS_{HMin}(EDT(i, j), h)) \quad (15)$$

From equations (14) and (15), segmented results are obtained that form the basis for detecting and diagnosing disease in an accurate and precise manner.

### Algorithm 2 Fully Convolution-based Watershed Segmentation

Input: Dataset ‘DS’

Output: Accurate cell pattern segmentation

Step 1: Initialize ‘n’, ‘k = 3 \* 3’, ‘s’, ‘s = 1’, ‘h = (1.0, 1.25, 1.5, 1.75, 2.0, 2.5, 3.0, 4.0, 5.0)’

Step 2: Begin

Step 3: For each Dataset ‘DS’ with preprocessed image ‘PI’

//Fully convoluted

Step 4: Perform convolution by applying Toeplitz matrix as given in equation (11)

Step 5: Perform pooling with the convoluted results as given in equation (12)

//Activation

//Segmentation

Step 6: Formulate Euclidean Distance Transform as given in equation (13)

Step 7: Evaluate normalized space results as given in equation (14) [separate region of interest from background tissues]

Step 8: Evaluate morphological watershed transform as given in equation (15) [separate nuclei from cytoplasm]

Step 9: Return segmented result ‘SRes’

Step 10: End for

Step 11: End

In algorithm 2, with the preprocessed image as input, the entire part is split to full convolution and segmentation. Segmentation comes under activation so improving overall cell pattern segmentation precision recall rate in an extensive manner.

## 4. Experimental Setup

Experimental evaluation of the proposed MPPI-FCWS to detect cancer with histology analysis and two existing methods, deep neural networks [1] and Deep Learning-based Segmentation [2], is implemented in Python high-level, general-purpose programming language. The dataset used in this work is the Breast Cancer Histology image dataset acquired from <https://www.kaggle.com/code/paultimothymooney/predict-idc-in-breast-cancer-histology-images>.

## 5. Implementation Details

We developed a method called MPPI-FCWS for detecting cancer via histology analysis with improved precision, recall, accuracy and minimal error rate.

- The MPPI-FCWS method comprises preprocessing and segmentation.
- The MPPI-FCWS method is compared with two existing methods, deep neural networks [1] and Deep Learning-based Segmentation [2], using a breast cancer histology dataset to validate the results.
- Initially, raw breast cancer histology images were obtained from the input dataset.
- Statistical Nucleic Normalized Moore Penrose Pseudoinverse Matrix-based preprocessing algorithm is employed to ensure normalized and denoised images from the raw input breast cancer histology dataset. Next, with the aid of statistical nucleic-based normalization Moore Penrose Pseudoinverse Matrix based denoising, preprocessed image with error minimized preprocessed sample results are obtained.

- A fully Convolution-based Watershed Segmentation algorithm is applied to separate regions of interest from background tissues and separate nuclei from the cytoplasm, so ensuring the accuracy of cell-pattern segmented results.

## 6. Discussion

Performance analysis of the proposed method, MPPI-FCWS, for detecting cancer via histology analysis is validated and analyzed by making a fair comparison between deep neural networks [1] and Deep Learning-based Segmentation [2]. To ensure fair comparison same dataset with similar sample images is used for providing detailed discussion.

### 6.1. CASE 1: Precision Analysis

Precision refers to the samples considered for simulation that were predicted correctly is denoted in the form of the model precision score. Precision analysis is also referred to as the positive predictive score analysis. It is evaluated as given below.

$$Precision = \frac{TP}{TP+FP} \tag{16}$$

From equation (16), precision ‘Pre’ is measured with the aid of the true positive rate ‘TP’ (i.e., detection of cancerous patient as cancer) and false positive rate ‘FP’ (i.e., detection of non-cancerous as cancerous patients). The compared results of the MPPI-FCWS method, deep neural networks [1] and deep learning-based segmentation [2] are shown in Table 2. From Table 2, experimental results show the precision rate of the MPPI-FCWS method is better than [1] and [2]. The precision results are trained for 10 iterations to evaluate its effectiveness in diagnosing breast cancer. The analysis reveals that with an increasing number of iterations, there is a corresponding decrease in precision rate, coupled with a gradual improvement. However, the analysis also demonstrates that the precision rate neither increases nor decreases throughout the training process.

Table 2. Comparison of precision results of different methods applied to the breast cancer histology image dataset

Samples	Precision		
	MPPI-FCWS	Deep Neural Networks	Deep Learning-based Segmentation
1500	0.86	0.83	0.8
3000	0.84	0.82	0.78
4500	0.82	0.8	0.76
6000	0.81	0.78	0.74
7500	0.8	0.78	0.74
9000	0.8	0.79	0.75
10500	0.82	0.8	0.77
12000	0.83	0.81	0.79
13500	0.82	0.81	0.79
15000	0.8	0.78	0.75

This is inferred from the simulation analysis with 1500 samples provided as input, 150 samples being detected with cancerous cell pattern, and 1350 samples detected with non-cancerous cell pattern, the true positive using the three methods MPPI-FCWS method, [1] and [2] were observed to be 130, 1250 and 120 and the false positive rate were observed to be 20, 25 and 30 respectively. With this, the overall precision rate was found to be 0.86, 0.83 and 0.80, respectively. The reason behind the improvement was owing to the application of the convolution employing the Toeplitz matrix for the preprocessed image provided as input. Followed by which the pooling with a kernel size of ‘3 \* 3’ was performed to obtain the pooled results. This, in turn, reduced false positives and improved true positives significantly, therefore improving overall precision using MPPI-FCWS by 3% and 7% than the [1] and [2].

### 6.2. CASE 2: Recall Analysis

Recall analysis is made that evaluates the method’s accuracy in predicting positives as differentiated from actual positives and is measured by the model recall score. This specifically differs from the precision that takes into consideration how many of the total number of positive predictions produced by the models are truly positive. With this recall analysis, the method's potential to identify positive instances is indicated by a high recall score. Recall is evaluated using the formula given below.

$$Recall = \frac{TP}{TP+FN} \tag{17}$$

From equation (17), recall rate ‘Rec’, is evaluated by taking into consideration the true positive rate ‘TP’ and false negative rate ‘FN’

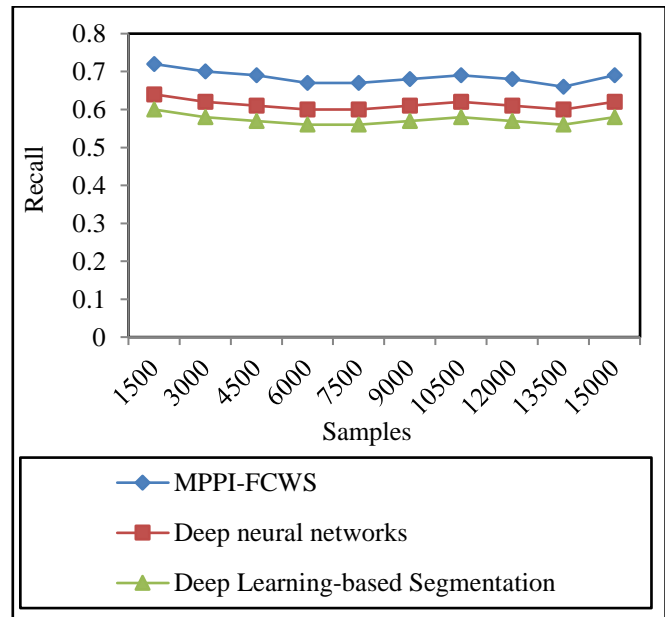


Fig. 4 Comparison of recall rate using MPPI-FCWS, Deep Neural Networks [1] and Deep Learning-based Segmentation [2]

A comparison between the proposed MPPI-FCWS method and existing related studies [1] and [2] analyzing recall rate is shown in Figure 4. Also, the recall rate using the proposed MPPI-FCWS method was found to be comparatively lesser than [1] and [2]. This showed an improvement in terms of recall rate. The improvement of the recall rate using the proposed MPPI-FCWS method is owing to the application of a Fully Convolution-based Watershed Segmentation algorithm.

By applying this algorithm initially, the preprocessed image was provided as input to the full convolution part, where convoluted results were obtained using the Toeplitz matrix, and pooled results were formed with respect to the kernel size of '3 \* 3' performed to obtain the pooled results. The convolution here represented the area of overlap under the pooled vectors, also by applying this pooling that in turn minimizes the feature map resolution without compromising the contrast. With this, the false negative using the three methods were observed to be 50, 70 and 80. This confirmed overall recall rate improvement using MPPI-FCWS by 12% and 20% than the [1, 2].

### 6.3. CASE 3: Accuracy Analysis

Third, in this section, the method accuracy is mathematically defined as the ratio of true positive 'TP' and true negative 'TN' to all the positive and negative observations, amounting to one of the most extensively utilized performance factors for learning segmentation models. The accuracy rate is mathematically solved using the formula given below.

$$Accuracy = \frac{TP+TN}{TP+TN+FP+FN} \quad (18)$$

From the above equation (18), the accuracy rate 'Acc' measures the number of times and learning method predicted the cancer detection result accurately out of all the segmented cell patterns it made. The compared results of the MPPI-FCWS method, deep neural networks [1] and deep learning-based segmentation [2] with respect to accuracy rate substituting the formulates from equation (18) are shown in Table 3.

From Table 3 the experimental results show that the accuracy rate of the proposed MPPI-FCWS method is found to be comparatively better than [1] and [2]. The accuracy results were trained for 10 iterations to measure its efficiency in diagnosing breast cancer based on cell patterns.

The analysis infers that with an increasing number of sample images, the corresponding decrease in accuracy rate was observed, coupled with a gradual improvement. The analysis also demonstrates that the accuracy rate neither increases nor decreases throughout the training process, and this, in turn, infers that increasing the number of samples will not affect the accuracy rate.

**Table 3. Comparison of accuracy results of different methods applied to the breast cancer histology image dataset**

Samples	Accuracy (%)		
	MPPI-FCWS	Deep Neural Networks	Deep Learning-based Segmentation
1500	0.95	0.93	0.92
3000	0.93	0.89	0.83
4500	0.91	0.87	0.81
6000	0.9	0.85	0.8
7500	0.88	0.83	0.79
9000	0.85	0.81	0.77
10500	0.85	0.81	0.73
12000	0.87	0.82	0.75
13500	0.89	0.83	0.77
15000	0.89	0.84	0.78

This is inferred from the simulation analysis with 1500 samples provided as input, 150 samples being detected with cancerous cell pattern and 1350 samples detected with non-cancerous cell pattern; the accuracy rate using the three methods MPPI-FCWS method, [1] and [2] were observed to be 95%, 93% and 92% respectively. The reason for accuracy improvement using the MPPI-FCWS method was due to the application of a Fully Convolution-based Watershed Segmentation algorithm. With this algorithm, the activation of the full convolution was performed by means of H-minima transform-based Watershed Segmentation. In addition, the preprocessed image serving as the markers and the pooled values serving as the nuclei mask were applied with Euclidean Distance Transform to separate regions of interest from background tissues and separate nuclei from the cytoplasm. This, in turn, segmented the cell patterns in an accurate manner, therefore improving the overall accuracy using the MPPI-FCWS method by 5% compared to [1] and 12% compared to [2], respectively.

### 6.4. Case 4: Error Rate Analysis

Error rate analysis usually infers the method's efficiency in detecting cancerous and differentiating between cancerous and non-cancerous based on cell pattern segmented portions. The lower the error rate more efficient the method is said to be, and vice versa. It is evaluated as given below.

$$Error\ Rate = \sum_{i=1}^n \frac{SI_{WD}}{SI_i} * 100 \quad (19)$$

From the above equation (19) results, the error rate analysis is made 'ER' by taking into consideration the sample images 'SI<sub>i</sub>' involved in the simulation process and the sample images wrongly detected results. 'SI<sub>WD</sub>' into consideration. It is measured in terms of percentage (%). Figure 5 shows a graphical representation of error rate analysis MPPI-FCWS, deep neural networks [1] and Deep Learning-based Segmentation [2]. From the below figure, an increase in the error rate using all three methods is observed for an increase in sample size.

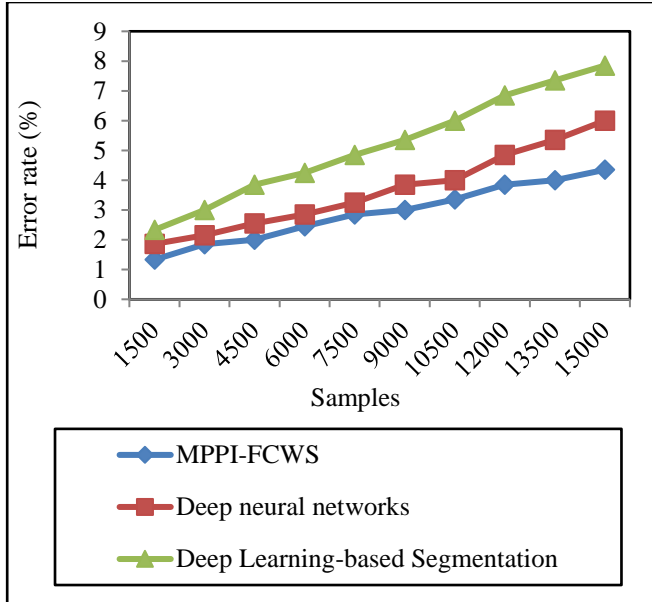


Fig. 5 Comparison of error rate using MPPI-FCWS, deep neural networks [1] and deep learning-based segmentation [2]

To detect cancer based on cell pattern segmentation with histology analysis for cancer grading, accurate and precise analysis has to be made so that the error involved in the overall analysis can be minimized. From the above figure, the error rate using the MPPI-FCWS method was found to be 1.33%, whereas using [1] and [2] was observed to be 1.86% and 2.33%, respectively. From these results, the error rate performance analysis using the MPPI-FCWS method was comparatively better than [1] and [2]. The reason was due to the application of the Statistical Nucleic Normalized Moore Penrose Pseudoinverse Matrix-based preprocessing algorithm. By applying this algorithm, the first normalization was performed using the statistic nucleic model, and then denoising was performed with the normalized images using the Moore Penrose Pseudoinverse Matrix. This, in turn, aided in accurate and precise cancer grading to differentiate between cancerous and non-cancerous. With this overall error rate using the MPPI-FCWS method was reduced by 20% and 43% than the [1, 2].

### 6.5. Comparison of Proposed and State-Of-Art Works

In this section, performance analysis of the proposed MPPI-FCWS method, deep neural networks [1] and Deep Learning-based Segmentation [2] are compared with the

## References

- [1] Frauke Wilm et al., "Pan-Tumor T-Lymphocyte Detection using Deep Neural Networks: Recommendations for Transfer Learning in Immunohistochemistry," *Journal of Pathology Informatics*, vol. 43, 2023. [CrossRef] [Google Scholar] [Publisher Link]
- [2] Daisuke Komura et al., "Restaining-Based Annotation for Cancer Histology Segmentation to Overcome Annotation-Related Limitations Among Pathologists," *Patterns*, vol. 4, no. 2, pp. 1-18, 2023. [CrossRef] [Google Scholar] [Publisher Link]
- [3] Mio Yamaguchi et al., "Automatic Breast Carcinoma Detection in Histopathological Micrographs based on Single Shot Multibox Detector," *Journal of Pathology Informatics*, vol. 13, 2022. [CrossRef] [Google Scholar] [Publisher Link]

Breast Cancer Histology image dataset. The evaluation is conducted using various metrics, such as precision, recall, accuracy and error rate. Table 4, given below, summarizes the results of the MPPI-FCWS method [1], [2]. Table 4 demonstrates the overall performance results of all parameters, including precision, recall, accuracy, and error rate, for three methods. The results of the proposed MPPI-FCWS method are provided to better performance of precision, recall and accuracy by 0.82, 0.69 and 0.89 compared to the existing methods. Also, the average error rate is reduced by up to 2.9% using the proposed MPPI-FCWS method compared to state-of-the-art works.

Table 4. Overall results of the proposed MPPI-FCWS method, state-of-art works such as deep neural networks [1] and Deep learning-based segmentation [2] Breast cancer histology image dataset

Methods/Metrics	Proposed MPPI-FCWS	Existing Deep Neural Networks	Existing Deep Learning-based Segmentation
Precision	0.82	0.8	0.77
Recall	0.69	0.61	0.57
Accuracy	0.89	0.84	0.79
Error rate (%)	2.9	3.67	5.16

## 7. Conclusion

Breast cancer detection cannot be precisely predicted by simply investigating discrete causes of disease. Only through the construction of a considerable analysis can histopathologists be provided with predictions of highly probable diseases. Past research works focused on cancer detection with histology analysis both using traditional and non-traditional methods, including machine learning and deep learning. In this work, significant deep learning using MPPI-FCWS to detect cancer with histology analysis is proposed with the objective of improving detection. The simulation consequences validated that the MPPI-FCWS method provides better results in precision, recall, accuracy and error rate overhead compared to existing methods.

## Data Availability

Data are available within the article. The data have been gathered from (<https://www.kaggle.com/code/paultimothymooney/predict-idc-in-breast-cancer-histology-images>)

- [4] Musa Adamu Wakili et al., “Classification of Breast Cancer Histopathological Images Using DenseNet and Transfer Learning,” *Computational Intelligence and Neuroscience*, vol. 2022, no. 1, pp. 1-31, 2022. [[CrossRef](#)] [[Google Scholar](#)] [[Publisher Link](#)]
- [5] Nadia Brancati et al., “BRACS: A Dataset for BReAst Carcinoma Subtyping in H&E Histology Images,” *Database: The Journal of Biological Databases and Curation*, vol. 2022, pp. 1-10, 2022. [[CrossRef](#)] [[Google Scholar](#)] [[Publisher Link](#)]
- [6] Yiping Zhou, Can Zhang, and Shaoshuai Gao, “Breast Cancer Classification from Histopathological Images Using Resolution Adaptive Network,” *IEEE Access*, vol. 10, pp. 35977-35991, 2022. [[CrossRef](#)] [[Google Scholar](#)] [[Publisher Link](#)]
- [7] Mahati Munikoti Srikantamurthy et al., “Classification of Benign and Malignant subtypes of Breast Cancer Histopathology imaging using Hybrid CNN-LSTM based Transfer Learning,” *BMC Medical Imaging*, vol. 23, no. 19, pp. 1-15, 2023. [[CrossRef](#)] [[Google Scholar](#)] [[Publisher Link](#)]
- [8] Chuang Zhu et al., “Breast Cancer Histopathology Image Classification through Assembling Multiple Compact CNNs,” *Medical Informatics and Decision Making*, vol. 19, no. 19, pp. 1-19, 2019. [[CrossRef](#)] [[Google Scholar](#)] [[Publisher Link](#)]
- [9] Ahsan Rafiq et al., “Detection and Classification of Histopathological Breast Images Using a Fusion of CNN Frameworks,” *Diagnostics*, vol. 13, no. 10, pp. 1-19, 2023. [[CrossRef](#)] [[Google Scholar](#)] [[Publisher Link](#)]
- [10] Y. Wang et al., “Improved Breast Cancer Histological Grading using Deep Learning,” *Annals of Oncology*, vol. 33, no. 1, pp. 89-98, 2023. [[CrossRef](#)] [[Google Scholar](#)] [[Publisher Link](#)]
- [11] Weijian Tao et al., “A Fusion Deep Learning Framework based on Breast Cancer Grade Prediction,” *Digital Communications and Networks*, vol. 10, no. 6, pp. 1782-1789, 2023. [[CrossRef](#)] [[Google Scholar](#)] [[Publisher Link](#)]
- [12] Santisudha Panigrahi et al., “Classifying Histopathological Images of Oral Squamous Cell Carcinoma using Deep Transfer Learning,” *Heliyon*, vol. 9, no. 3, pp. 1-14, 2023. [[CrossRef](#)] [[Google Scholar](#)] [[Publisher Link](#)]
- [13] Eatedal Alabdulkreem et al., “Bone Cancer Detection and Classification Using Owl Search Algorithm with Deep Learning on X-Ray Images,” *IEEE Access*, vol. 11, pp. 109095-109103, 2023. [[CrossRef](#)] [[Google Scholar](#)] [[Publisher Link](#)]
- [14] Gabriel Jiménez, and Daniel Racoceanu, “Deep Learning for Semantic Segmentation vs. Classification in Computational Pathology: Application to Mitosis Analysis in Breast Cancer Grading,” *Frontiers in Bioengineering and Biotechnology*, vol. 7, pp. 1-12, 2019. [[CrossRef](#)] [[Google Scholar](#)] [[Publisher Link](#)]
- [15] Kyubum Lee et al., “Deep Learning of Histopathology Images at the Single Cell Level,” *Frontiers in Artificial Intelligence*, vol. 4, pp. 1-14, 2021. [[CrossRef](#)] [[Google Scholar](#)] [[Publisher Link](#)]
- [16] Sameen Aziz et al., “IVNet: Transfer Learning Based Diagnosis of Breast Cancer Grading Using Histopathological Images of Infected Cells,” *IEEE Access*, vol. 11, pp. 127880-127894, 2023. [[CrossRef](#)] [[Google Scholar](#)] [[Publisher Link](#)]
- [17] Faisal Bin Ashraf, S.M. Maksudul Alam, and Shahriar M. Saki, “Enhancing Breast Cancer Classification Via Histopathological Image Analysis: Leveraging Self-Supervised Contrastive Learning and Transfer Learning,” *Heliyon*, vol. 10, no. 2, pp. 1-10, 2024. [[CrossRef](#)] [[Google Scholar](#)] [[Publisher Link](#)]
- [18] C. van Doonijeweert, P.J. van Diest, and I.O. Ellis, “Grading of Invasive Breast Carcinoma: The Way Forward,” *Virchows Archiv*, vol. 480, no. 1, pp. 33-43, 2021. [[CrossRef](#)] [[Google Scholar](#)] [[Publisher Link](#)]
- [19] Michal Karol et al., “Deep Learning for Cancer Cell Detection: Do We Need Dedicated Models?,” *Artificial Intelligence Review*, vol. 57, no. 3, pp. 1-36, 2023. [[CrossRef](#)] [[Google Scholar](#)] [[Publisher Link](#)]
- [20] Tanzila Saba, “Recent Advancement in Cancer Detection using Machine Learning: Systematic Survey of Decades, Comparisons and Challenges,” *Journal of Infection and Public Health*, vol. 13, no. 9, pp. 1274-1289, 2020. [[CrossRef](#)] [[Google Scholar](#)] [[Publisher Link](#)]
- [21] Ali Hasan Md. Linkon et al., “Deep Learning in Prostate Cancer Diagnosis and Gleason Grading in Histopathology Images: An Extensive Study,” *Informatics in Medicine Unlocked*, vol. 24, 2021. [[CrossRef](#)] [[Google Scholar](#)] [[Publisher Link](#)]
- [22] Nina Youneszade, Mohsen Marjani, and Chong Pei Pei, “Deep Learning in Cervical Cancer Diagnosis: Architecture, Opportunities, and Open Research Challenges,” *IEEE Access*, vol. 11, pp. 6133-6149, 2023. [[CrossRef](#)] [[Google Scholar](#)] [[Publisher Link](#)]
- [23] Taye Girma Debelee et al., “Deep Learning in Selected Cancers’ Image Analysis-A Survey,” *Journal of Imaging*, vol. 6, no. 11, pp. 1-40, 2021. [[CrossRef](#)] [[Google Scholar](#)] [[Publisher Link](#)]
- [24] Marit Lucas et al., “Deep Learning for Automatic Gleason Pattern Classification for Grade Group Determination of Prostate Biopsies,” *Virchows Archiv*, vol. 485, no. 1, pp. 77-85, 2019. [[CrossRef](#)] [[Google Scholar](#)] [[Publisher Link](#)]
- [25] R. Rashmi, Keerthana Prasad, and Chethana Babu K Udupa, “Breast Histopathological Image Analysis using Image Processing Techniques for Diagnostic Purposes: A Methodological Review,” *Journal of Medical Systems*, vol. 46, no. 7, pp. 1-24, 2021. [[CrossRef](#)] [[Google Scholar](#)] [[Publisher Link](#)]
- [26] Andrew Su et al., “A Deep Learning Model for Molecular Label Transfer that Enables Cancer Cell Identification from Histopathology Images,” *Precision Oncology*, vol. 6, no. 14, pp. 1-11, 2022. [[CrossRef](#)] [[Google Scholar](#)] [[Publisher Link](#)]
- [27] Suzanne C. Wetstein et al., “Deep Learning-Based Breast Cancer grading and Survival Analysis on Whole-Slide Histopathology Images,” *Scientific Reports*, vol. 12, no. 1, pp. 1- 12, 2022. [[CrossRef](#)] [[Google Scholar](#)] [[Publisher Link](#)]
- [28] Khoa A. Tran et al., “Deep Learning in Cancer Diagnosis, Prognosis and Treatment Selection,” *Genome Medicine*, vol. 13, no. 1, pp. 1-17, 2021. [[CrossRef](#)] [[Google Scholar](#)] [[Publisher Link](#)]

- [29] Piyush Gupta et al., "Prediction of Health Monitoring with Deep Learning using Edge Computing," *Measurement: Sensors*, vol. 25, 2023. [[CrossRef](#)] [[Google Scholar](#)] [[Publisher Link](#)]
- [30] Roseline Oluwaseun Ogundokun et al., "Medical Internet-of-Things Based Breast Cancer Diagnosis Using Hyperparameter-Optimized Neural Networks," *Future Internet*, vol. 14, no. 5, pp. 1-20, 2022. [[CrossRef](#)] [[Google Scholar](#)] [[Publisher Link](#)]
- [31] Muhammad Umer et al., "Breast Cancer Detection Using Convolved Features and Ensemble Machine Learning Algorithm," *Cancers*, vol. 14, no. 23, pp. 1-18, 2022. [[CrossRef](#)] [[Google Scholar](#)] [[Publisher Link](#)]
- [32] Bitao Jiang et al., "Deep Learning Applications in Breast Cancer Histopathological Imaging: Diagnosis, Treatment, and Prognosis," *Breast Cancer Research*, vol. 26, no. 1, pp. 1-17, 2024. [[CrossRef](#)] [[Google Scholar](#)] [[Publisher Link](#)]
- [33] Deepa Kumari et al., "Predicting Breast Cancer Recurrence using Deep Learning," *Discover Applied Sciences*, vol. 7, no. 2, pp. 1-33, 2025. [[CrossRef](#)] [[Google Scholar](#)] [[Publisher Link](#)]
- [34] Andrew Janowczyk, and Anant Madabhushi, "Deep Learning for Digital Pathology Image Analysis: A Comprehensive Tutorial with Selected Use Cases," *Journal of Pathology Informatics*, vol. 7, no. 1, 2016. [[CrossRef](#)] [[Google Scholar](#)] [[Publisher Link](#)]
- [35] Angel Cruz-Roa et al., "Automatic Detection of Invasive Ductal Carcinoma in Whole Slide Images with Convolutional Neural Networks," *Proceedings of SPIE, the International Society for Optical Engineering*, San Diego, California, United States, vol. 9041, 2014. [[CrossRef](#)] [[Google Scholar](#)] [[Publisher Link](#)]